

LIDAR DATA SEGMENTATION AND CLASSIFICATION BASED ON OCTREE STRUCTURE

Miao Wang^a, Yi-Hsing Tseng^b

Department of Geomatics, National Cheng Kung University, No.1 University Road, Tainan 701, Taiwan, R.O.C.

^a monsterr@seed.net.tw

^b tseng@mail.ncku.edu.tw

KEY WORDS: Lidar, Laser Scanning, Feature Extraction, Organization, Segmentation, Classification

ABSTRACT:

Lidar (or laser scanning) has become a viable technique for the collection of a large amount of accurate 3D point data densely distributed on the scanned object surface. The inherent 3D nature of the sub-randomly distributed point cloud provides abundant spatial information. To explore valuable spatial information from laser scanned data becomes an active research topic. The sub-randomly distributed point cloud should be segmented and classified before the extraction of spatial information and the first step in the processing of the spatial data extraction is an organization of the lidar data. This paper proposes a new algorithm to split and merge the lidar data based on the octree structure. After the process a lidar data set can be segmented to 3D plane clusters and classified by the plane attributes derived from each 3D plane, such as area, gradient, intensity etc. Some example and analysis of practical data set will be performed for segmentation and classification using the proposed methods here. The test result shows the potential of applying this method to extracting spatial information from lidar data.

1. INTRODUCTION

Lidar (or laser scanning) has become a viable technique in recent decades. The ability of collecting a large amount of accurate 3D point data densely distributed on the scanned object surface has brought us a new research topic (Ackermann, 1999). The inherent 3D nature of the sub-randomly distributed point cloud contains abundant space information and can be further extracted for digital elevation model generation, 3D building model reconstruction, and trees detection (Haala and Brenner, 1999; Maas and Vosselman, 1999; Priestnall, et al., 2000; Vosselman and Dijkman, 2001). To explore valuable spatial information from lidar data becomes an active topic.

Lidar data record 3D surface information in detail. To explore valuable spatial information from the huge amount of 3D data is difficult and time consuming. Segmentation is generally prerequisite for spatial feature extracting. Most segmentation techniques were developed from 2.5D grid data or image data (Masaharu and Hasegawa, 2000; Geibel and Stilla, 2000). Sub-randomly distributed point cloud is transformed into a grid data set through an interpolation procedure to apply an image-based segmentation and Classification (S/C), but some important spatial information may be lost (Axelsson, 1999; Gamba and Casella, 2000). Eventually, new S/C methods suitable for lidar data are needed for practical application.

An octree-structure-based split-and-merge segmentation method for organizing lidar point cloud into clusters of 3D planes is proposed here. The method is hierarchically splitting the point cloud set on the octree structure until the points contained in each sub-node are coplanar, or say distributed in a 3D plane or less than 3 points. The neighbouring 3D planes with similar attribute are merged after splitting to form larger planes.

The segmented 3D planes than can be classified according to the attributes derived from each 3D plane. The proposed method would suitably work for airborne lidar data as well as

ground-based laser scanning data. Some results on both kind of lidar are presented in this paper finally.

2. OCTREE-STRUCTURE-BASED SEGMENTATION

The principle of the method is to segment point cloud into 3D planes. A split and merge segmentation based on the octree structure (Fig. 1.a) is developed.

2.1 Split process

The split process starts from the whole data set as a root node. The data set space will be divided into 8 equal sub-spaces, if the data set could not pass the distance and area threshold. The split generates 8 sub-nodes (Figure 1.b) representing the split spaces. Each sub-node will be split continuously until the scan points contained in the split space of the sub-node are distributed close to a 3D best-fit plane or less than 3 points.

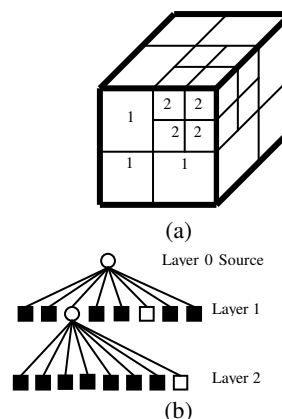


Figure 1. Octree structure (a) divided sub-spaces (b) the tree representation

2.2 Calculating best-fit planar of point cloud

The best-fit plane in each sub-node is determined using least-squares estimation, i.e., minimizing the squares sum of the distances from points to the fitting plane. In the 3D Euclid space, a 3D plane can be formulated as follows:

$$Ax + By + Cz + D = 0 \quad (1)$$

The distance (d_i) from the i^{th} point $P_i(x_i, y_i, z_i)$ to the plane can be expressed as:

$$d_i = \frac{|Ax_i + By_i + Cz_i + D|}{\sqrt{A^2 + B^2 + C^2}} \quad (2)$$

Then, the best-fit condition of minimizing the squares sum of the distances will be:

$$\sum_{i=1}^N d_i^2 \Rightarrow \min \quad (3)$$

Eq. (2) is non-linear, so that it needs initial approximation values of the unknown parameters (A, B, C, D) for the calculation of least-squares estimation. To solve this problem, we use a two-stage calculation to determine the unknown parameters.

At first stage, a 3D plane is formulated as a slope-intercept form, which has 3 types as Eq. (4):

$$\begin{aligned} x &= ay + bz + c \\ y &= ax + bz + c \\ z &= ax + by + c \end{aligned} \quad (4)$$

To avoid the situation of obtaining infinite numbers for a and b parameters, which slope-intercept form is suitable can be predetermined according to the distribution ranges of the point cloud. Figure 2 shows the idea. The outer frames in Fig. 2 represent the sub-node spaces, and the inner frames represent the distribution ranges of the point cloud. The decision can be done by checking the minimum distribution range. For example, if x dimension has the minimum distribution range, then the first type is the choice.

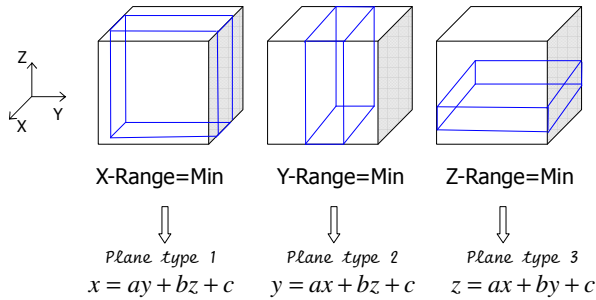


Figure 2. The ideas of selecting a suitable slope-intercept form.

Because the slope-intercept form is linear, the parameters can be calculated without the need of iteration. The least-squares linear regression can be applied to determine the plane parameters.

For example, if the slope-intercept form, $x = ay + bz + c$, is used, the matrix form of the observation equations can be listed as follows:

$$V = A \cdot X - L$$

$$\begin{bmatrix} v_1 \\ \vdots \\ v_i \\ \vdots \\ v_n \end{bmatrix} = \begin{bmatrix} y_1 & z_1 & 1 \\ \vdots & \vdots & \vdots \\ y_i & z_i & 1 \\ \vdots & \vdots & \vdots \\ y_n & z_n & 1 \end{bmatrix} \begin{bmatrix} a \\ b \\ c \end{bmatrix} - \begin{bmatrix} x_1 \\ \vdots \\ x_i \\ \vdots \\ x_n \end{bmatrix} \quad (5)$$

The parameters are then solved as:

$$\hat{X} = (A^T A)^{-1} A^T L \quad (6)$$

The calculation in this stage actually is to minimize the squares sum of the x ranges from points to the fitting plane rather the perpendicular distances. After the parameters are determined, the x range residuals can be calculated. Split will proceed continuously if there is a residual larger than the preset threshold, otherwise rigorous calculation of the second stage will be triggered.

Eq. 2 is applied for the rigorous calculation. Given the solution in the first stage as the initial approximation, the rigorous adjustment is performed iteratively. Following the use of the slope-intercept form, Eq. 2 can be reformed as:

$$d_i = F_i(a, b, c) = \frac{|-x_i + ay_i + bz_i + c|}{\sqrt{(-1)^2 + a^2 + b^2}} \quad (7)$$

The observation equations can be obtained by linearizing Eq. 7:

$$0 + v_i = \left[\frac{\partial F_i}{\partial a} \right]_0 \Delta a + \left[\frac{\partial F_i}{\partial b} \right]_0 \Delta b + \left[\frac{\partial F_i}{\partial c} \right]_0 \Delta c + F_0 \quad (8)$$

In Eq. 8, the parameters $\Delta a, \Delta b, \Delta c$ are increments of unknown parameters. The increments will be added into the previous approximations until the calculated increments get to very small. The best-fit plane is determined if the computation converges. The distance residuals can be calculated after the parameters are solved. Again, split will proceed continuously if there is a residual larger than the preset threshold, otherwise a plane is formed.

2.3 Area of the point cloud on a fitting plane

The point cloud in a sub-space may not distribute evenly on the sub-node. In order to find a suitable node size corresponding to the distributing of point cloud, area of the point cloud is checked for further splitting. For example, area of unbalanced distributing points in Figure 3 is smaller than the area of face of sub-node. Split can proceed further, until the area of distributing points on each fitting plane is larger than a preset threshold.

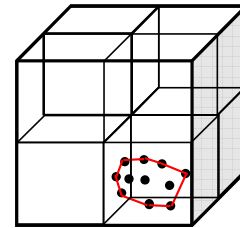


Figure 3. An example of unbalanced distribution of points

Point cloud of each best plane in sub-node is than searching its boundary and building its TIN for visual purpose. Figure 4 is the example of source lidar points cloud before split. Figure 5 a,

shows the result of split node border. Figure 5.b, c shows the best-fit plane of each split sub points set by its border and TIN respectively.

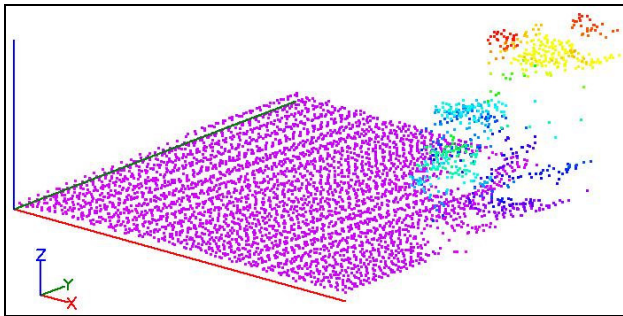
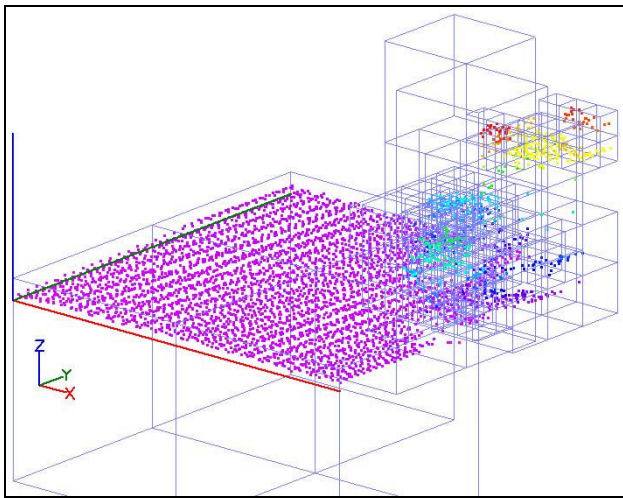
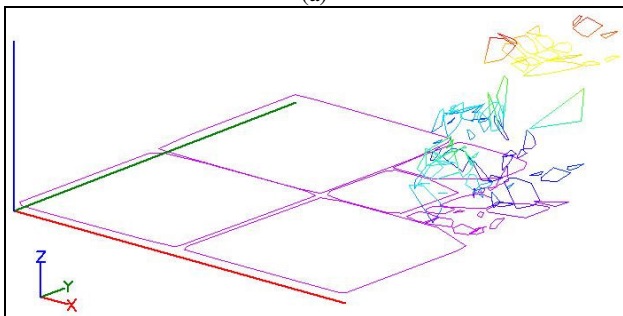


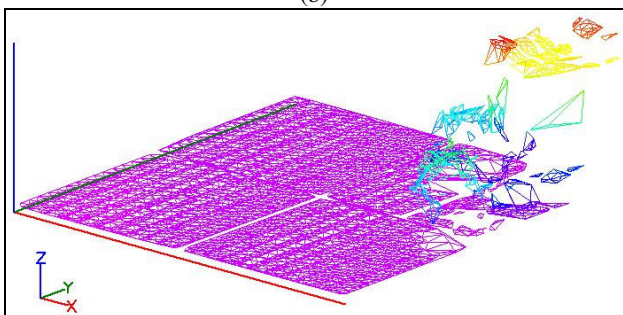
Figure 4. An example of source lidar point cloud.



(a)



(b)

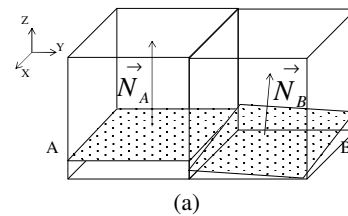


(c)

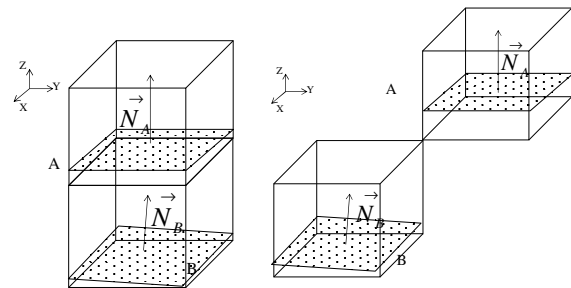
Table 5. Result of splitting (a) node border (b) best-fit plane border (c) best-fit plane TIN

2.4 Merge process

A merge process is then performed after splitting to reunite similar neighbouring planes. Each node in octree structure has 26 equal or larger neighbouring nodes at most. The octree structure allows us to find neighboring planes easily (Samet, H., 1990). When a neighboring plane is found, the merge process will first check whether their normal vectors are similar. Figure 6.a shows the idea of checking normal vectors. However, one may find planes in different layers having similar normal vectors (Figure 6.b). To solve this situation, additional check of the node relation is needed. After two neighboring planes are found similar, the rigorous calculation will be triggered again to recalculate the parameters of the merged plane and to ensure the merge availability. After the merge process, the original lidar point cloud was segmented into clusters of 3D planes. Each merged 3D plane can be recorded as 4 plane parameters (A, B, C, D) and its border points. A TIN (Triangular Irregular Network) of each plane is also generated for visualization use. Figure 7 a, b, shows the result of merged plane in the form of border and TIN. It is obviously that the 4 separated ground planes in Figure 5.b was merged into a larger plane successfully in Figure 7.b. after the merge process.

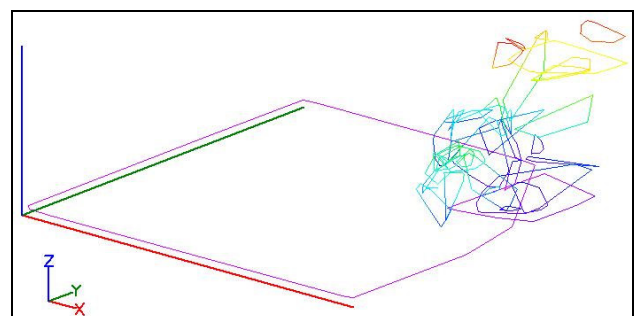


(a)



(b)

Figure 6. Similarity of two neighboring nodes A and B (a) available for merge (b) not available for merge



(a)

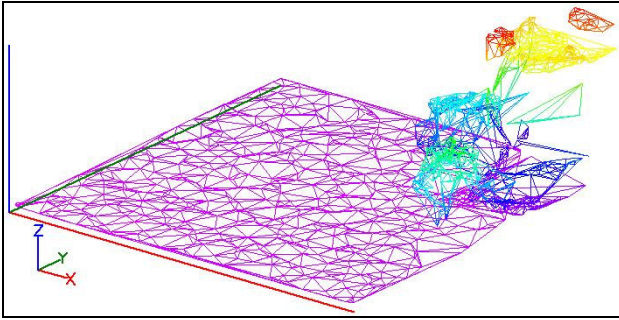
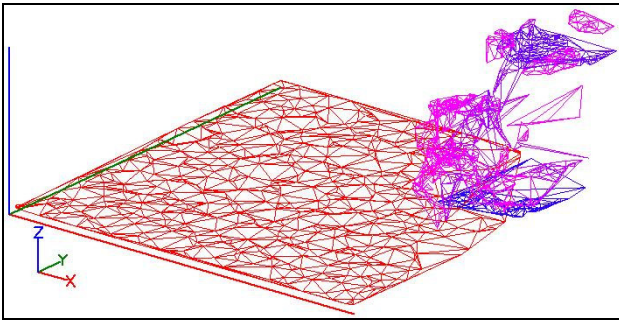


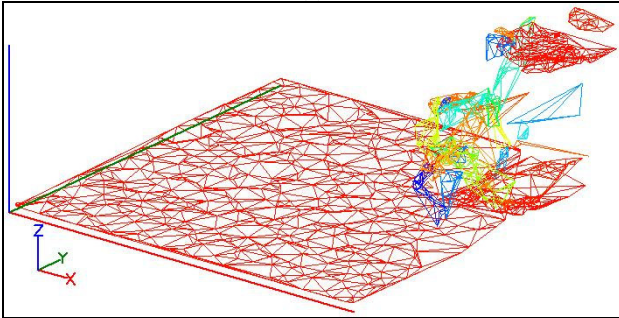
Figure 7 Result of merged plane (a) border (b) TIN

3. CLASSIFICATION

A classification can be performed based on the attributes of the extracted 3D planes. In the time of preparing this paper, we have not developed a well classification method yet. However, simple classification results based on plane attributes such as area, average height, gradient, average intensity, shape, orientation and symmetry shows the potential of the feature-based classification. Figure 8a, b, shows the results of plane classification by area and gradient respectively.



(a)



(b)

Figure 8. Results of plane classification by (a) area and (b) gradient

Some classification examples of both airborne lidar and ground-based laser scanning data are shown in next section.

4. EXAMPLES AND ANALYSIS

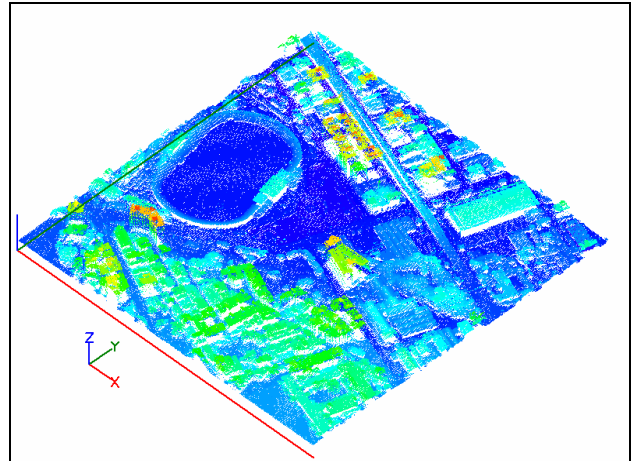
The proposed method can be applied to both airborne and ground lidar data. However, the thresholds used in the program should be adjusted to fit different data sets according to the different scanning accuracy. Our test data include an airborne lidar data set collected in Hsinchu, Taiwan with Leica ALS40 and a ground lidar data set obtained in The Eastern Gate of Hsinchu City with Optech ILRIS-3D laser scanner. Table 1 lists the basic data attributes and the thresholds applied in the tests.

	ALS40	ILRIS-3D
Scan Date	April 14 ,2002	February 16, 2004
Scan Area	Hsinchu	The Eastern Gate of Hsinchu City
Scan Accuracy	30 cm	0.7 cm
Point density	About 2.3pt/□	About 907pt/□
Point cloud size	515,991	464,563
Distance threshold	1m	0.05m
Area threshold	1/4 node face area	1/4 node face area
Angle threshold	3□	3□

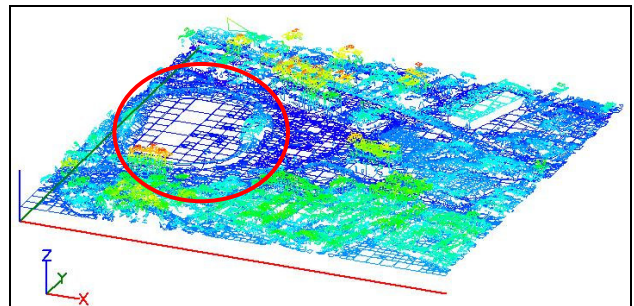
Table 1. Information of examples

4.1 Airborne lidar example

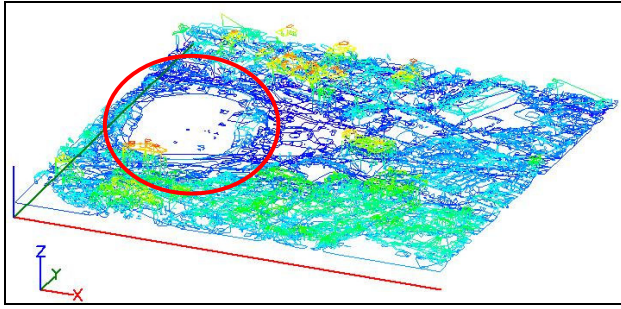
Figure 9.a shows a set of point cloud of airborne lidar covering an area of 500 x 500 m². Most of the points distribute densely over the ground surface and top of buildings, and points scatter on side wall of buildings are fewer. Figure 9.b shows the border of best-fit planes after the split process. Table 2 lists the computation time, the parameters of the octree structure, and the statistic data of extracted planes. In this case, 96.7% of the total points were used to form planes, the rest are scattered points which cannot be used to form planes. Figure 9.c shows the border of merged process. The stadium ground to the west is merged from pieces of planes. Figure 9.d, e, f, shows the results of merged plane classified by area, gradient, average intensity respectively. In Figure 9.e, vertical planes (building wall) and horizontal planes (building roof and ground) can be classified by their gradient.



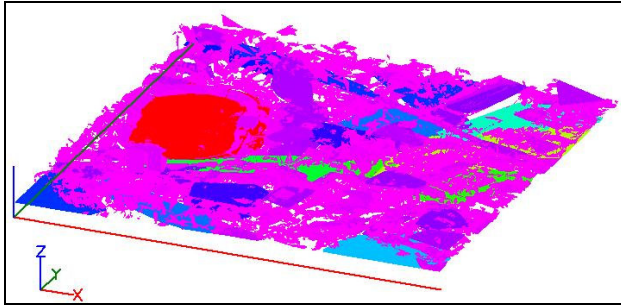
(a)



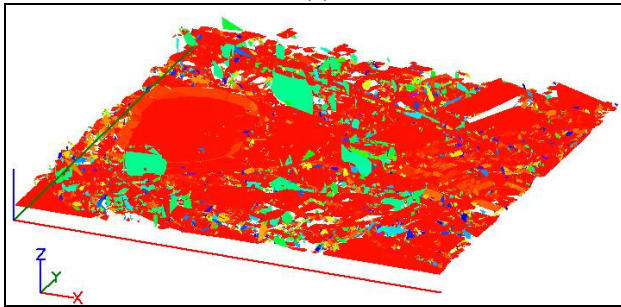
(b)



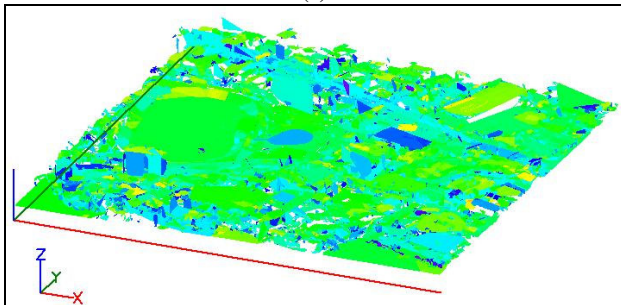
(c)



(d)



(e)



(f)

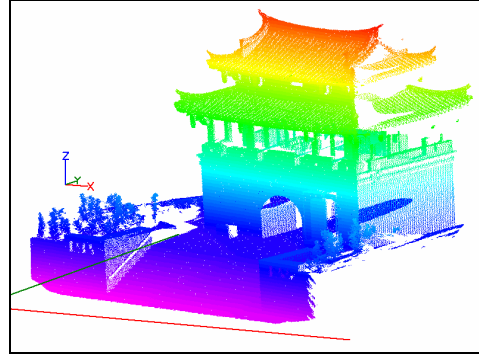
Figure 9. Airborne lidar example (a) point cloud (b) results after split (c) results after merge (d) classify by area (e) classify by Gradient (f) classify by average intensity

Computation time for split process	25.48 sec.
Computation time for merge process	403.132 sec
Number of the total octree layers	9
Number of the total leave nodes	42090
Extracted planes and % of the total points used	30013, 96.7%
Number of nodes have less than 3 points	12077

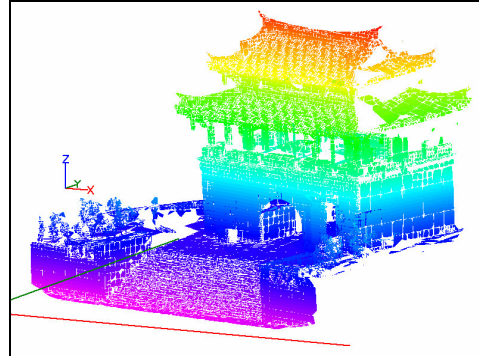
Table 2. Airborne laserscan information

4.2 Ground lidar example

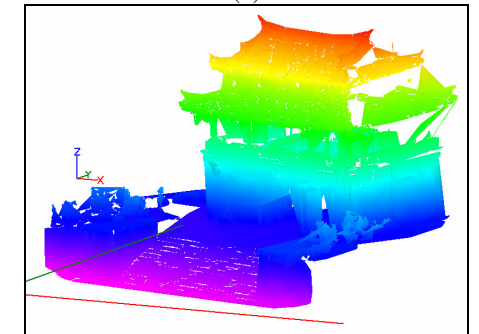
Figure 9.a shows the original point cloud of the ground lidar example. Extracted planes shown in Figure 9.b containing 98.7% of the total points. Figure 9.c shows the results after the merge process. Figure 9.d, e, f, shows the results of merged plane classified by area, gradient, average intensity respectively. In Figure 9.e horizontal planes and vertical planes of the stairs in front of the Gate can be classified obviously. Wall and roof of the Gate and ground plane can be classified too.



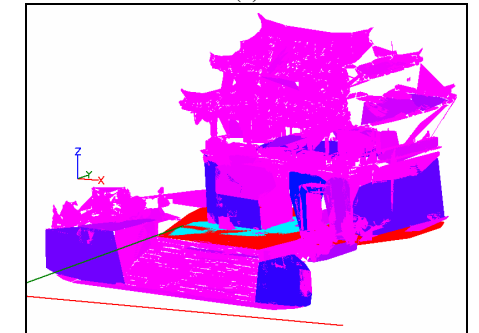
(a)



(b)



(c)



(d)

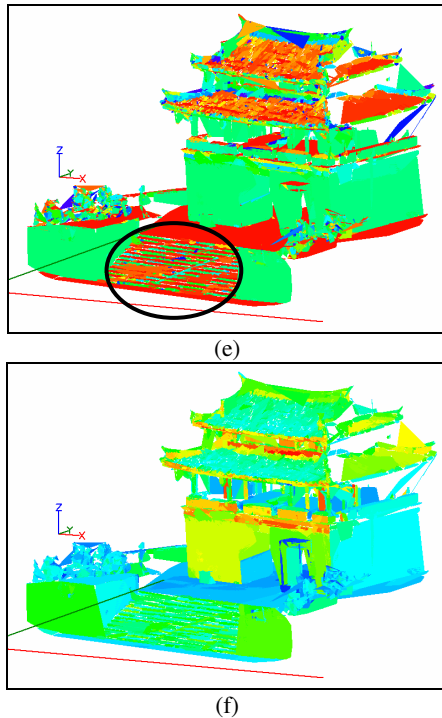


Fig . 9. Ground lidar example (a) point cloud (b) results after split (c) results after merge (d) classify by area (e) classify by Gradient (f) classify by average intensity

Computation time for split process	24.27 sec.
Computation time for merge process	360.96 sec.
Number of the total octree layers	10
Number of the total leave nodes	19803
Extracted planes and % of the total points used	10944, 98.7%
Number of nodes have less than 3 points	4323

Table 3. Ground laserscan information

5. CONCLUSIONS

Sub-randomly distributed point cloud of lidar data needs an ad hoc segmentation method for the extraction of spatial information. This paper proposes an octree-based split-and-merge segmentation method to divide lidar data into clusters of 3D planes and can apply to both airborne and ground lidar data. The thresholds designed in the algorithm can be adjusted to fit different data sets. We expect this segmentation method can be a stepping stone and applying to the other application of lidar data. For example:

- 3D Feature extraction and coordinate measurement --- 3D spatial geometric properties (line and point) can be explored by intersection of the extracted 3D planes.
- Building reconstruction --- extracted 3D features can be analyzed to reconstruct the building models.
- Classification – Attributes derived from 3D planes can be used to classify different meaningful information of planes.
- Data filtering and compression --- points were not used to form planes can be filtered out and densely distributed on a plane can be expressed by the 4 plane parameters and boundary to reduce data size.

Further study is needed to improve and modify the proposed method to fit various applications of both airborne and ground based lidar data.

REFERENCES

- Ackermann, F., 1999, Airborne Laser Scanning - Present Status and Future Expectations, *ISPRS Journal of Photogrammetry & Remote Sensing*, vol. 54, pp. 64-67.
- Axelsson, P., 1999, Processing of Laser Scanner Data - Algorithms and Applications, *ISPRS Journal of Photogrammetry & Remote Sensing*, vol. 54, pp. 138-147.
- Gamba, P. and V. Casella, 2000, Model Independent Object Extraction from Digital Surface Models, *Proc. International Archives of Photogrammetry and Remote Sensing*, Amsterdam.
- Geibel, R. and U. Stilla, 2000, Segmentation of Laser Altimeter Data for Building Reconstruction: Different Procedures and Comparison, *Proc. International Archives of Photogrammetry and Remote Sensing*, Amsterdam.
- Haala, N. and C. Brenner, 1999, Extraction of Building and Trees in Urban Environments, *ISPRS Journal of Photogrammetry & Remote Sensing*, vol. 54, pp. 130-137.
- Maas, H. G. and G. Vosselman, 1999, Two Algorithms for Extracting Building Models from Raw Laser Altimetry Data, *ISPRS Journal of Photogrammetry & Remote Sensing*, vol. 54, pp. 153-163.
- Masaharu, H. and H. Hasegawa, 2000, Three-Dimensional City Modeling from Laser Scanner Data by Extracting Building Polygons Using Region Segmentation Method, *Proc. International Archives of Photogrammetry and Remote Sensing*, Amsterdam.
- Priestnall, G., J. Jaafar and A. Duncan, 2000. Extracting Urban Features from LiDAR Digital Surface Models, *Computers, Environment and Urban Systems*, vol. 24, pp.65-78.
- Samet, H., 1990. Application of Spatial Data Structures: Computer Graphics, Image Processing, and GIS, *Addison-Wesley Publishing Company*, pp.57-110.
- Vosselman, G. and S. Dijkman, 2001, 3D Building Model Reconstruction from Point Clouds and Ground Plans, *Proc. International Archives of Photogrammetry and Remote Sensing*, Annapolis, Maryland.

ACKNOWLEDGEMENTS

The authors deeply appreciate the provision of the airborne Lidar data by the Council of Agriculture, Executive Yuan, R. O. C..